Cellular/Molecular

Firing-Pattern-Dependent Specificity of Cortical Excitatory Feed-Forward Subnetworks

Takeshi Otsuka and Yasuo Kawaguchi
Division of Cerebral Circuitry, National Institute for Physiological Sciences, Okazaki, Aichi 444-8787, Japan

The cortical circuit includes networks of highly interconnected pyramidal neurons. Here, we investigated whether pyramidal cells form subnetworks depending on pyramidal subtypes. We classified layer V (L5) pyramidal cells in rat frontal cortex into three physiological subtypes based on the presence (SA-d type) or absence (SA type) of an initial burst in neurons displaying slowly adapting spike trains, or fast spike frequency adaptation (FA type) against current pulse injections. Pyramidal cells projecting to the particular subcortical areas were correlated with the physiological subtypes. Focal glutamate stimulation of a L2/3 pyramidal cell induced EPSCs in SA and SA-d cells more frequently than in FA cells. FA cells in upper L5 received more inputs from the upper L2/3, and those in lower L5 received inputs from cells in lower L2/3, suggesting topographic interlaminar projections to FA cells. Dual recordings from L5 pyramidal cells revealed that common input probability that two L5 cells share inputs from a L2/3 cell was high in cell pairs of the same subtypes, compared with those in different subtype pairs. Furthermore, the common input probability was highly selective when cell pairs of the same subtypes, but not different subtypes, had connections between them. Our results suggest that L2/3 pyramidal cells selectively innervate L5 cells, depending on their firing subtypes.

Key words: **cortex; pyramidal cell; firing pattern; extracortical projection; connection specificity; interlaminar connection**

Introduction

The neocortex is a layered structure, and contains numerous types of excitatory and inhibitory neurons (DeFelipe and Fariñas, 1992; Kawaguchi and Kubota, 1997; Markram et al., 2004). Interlaminar excitatory connections are direction-selective, with the information originating in thalamic-receptive neurons transmitted first to excitatory neurons in superficial layers, and then relayed to deeper layers (Bureau et al., 2006; Lübke and Feldmeyer, 2007). As such a unit of cortical information processing, the cortex shows a columnar organization (Mountcastle, 1997). To facilitate the directional transfer of the information, pyramidal neurons selectively form synaptic connections. At finer scales within columns, the local circuitry can be divided into modules of selectively connected cells (Yoshimura et al., 2005). In layer V (L5) of the visual cortex, pairs of connected pyramidal cells are more likely to form connections to a third neuron than are unconnected pairs (Song et al., 2005). The divergent and convergent probabilities of interlaminar excitatory connections depend on the connectivity patterns of recipient and projecting cell pairs, respectively (Shepherd and Svoboda, 2005; Yoshimura et al., 2005; Kampa et al., 2006). These studies have been demonstrated that intralaminar and interlaminar connections of pyramidal cells are clustered into subnetworks.

Pyramidal cells, however, can be classified into several subtypes. Physiologically, cells firing burst of multiple spikes and regular spiking cells firing trains of single spikes during current pulse injection have been described (Connors et al., 1982; McCormick et al., 1985; Agmon and Connors, 1992; Cho et al., 2004). Pyramidal cells can be further classified based on the degree of the spike frequency adaptation during prolonged current injections (Gottlieb and Keller, 1997; Dégenètais et al., 2002; Chang and Luebke, 2007). Morphological analyses of dendritic branching patterns also revealed a diversity of pyramidal subtypes (Tsiola et al., 2003). In L5 pyramidal cells, a major source of subcortical projections, dendritic morphologies are correlated with their axonal projection targets and their firing patterns in some cortical areas (Chagnac-Amitai et al., 1990; Mason and Larkman, 1990; Hefti and Smith, 2000; Gao and Zheng, 2004; Morishima and Kawaguchi, 2006; Hattox and Nelson, 2007), suggesting that physiologically identified subtypes of L5 pyramidal cells sharing similar physiological characteristics represent functional output classes. Several studies have indicated that functional input-out connectivity of thalamocortical afferents and corticocortical connections differ between pyramidal subtypes (Agmon and Connors, 1992; Morishima and Kawaguchi, 2006; Schubert et al., 2006). However, it remains unknown whether these pyramidal subtypes form subnetworks.

Here, we investigated whether interlaminar connections from L2/3 to L5 pyramidal cells are segregated with regard to the subclass of L5 pyramidal cells. After quantitative identification of three firing subtypes among L5 pyramidal cells, we examined correlation of the firing subtypes with the subcortical projection

Received Sept. 8, 2008; accepted Sept. 20, 2008.

This work was supported by Grant-in-Aids for Scientific Research from the Ministry of Education, Culture, Sports, Science, and Technology (MEXT), Ministry of Health, Labor, and Welfare of Japan, the Uehara Memorial Foundation, and Brain Science Foundation to T.O. and Y.K. We thank A. Gulledge, T. Inoue, M. Morishima, M. Miyata, and Y. Kubota for helpful comments. We are grateful to M. Morishima for technical advice on the retrograde tracer experiment.

Correspondence should be addressed to Yasuo Kawaguchi, Division of Cerebral Circuitry, National Institute for Physiological Sciences, 5-1 Myodaiji-Higashiyama, Okazaki, Aichi 444-8787, Japan. E-mail: yasuo@nips.ac.jp.

DOI:10.1523/JNEUROSCI.1921-08.2008

 0270-6474/08/2811186-10$15.00/0

targets. We then investigated the spatial distribution of L2/3 cells innervating L5 pyramidal subtypes, and the divergence pattern from L2/3 to L5 cell pairs. Our results suggest that the interlaminar synaptic pathways originating from L2/3 are segregated according to L5 pyramidal subtypes, and that these subtype-dependent pathways are further segregated into modules of synaptically interconnected cells.

Materials and Methods

Whole-cell recordings in slice. All experiments were conducted in compliance with the guidelines for animal experimentation of the Okazaki National Research Institutes. Slices including frontal cortex were prepared from Wistar rats, aged postnatal day 19–23. Rats were anesthetized with isoflurane and decapitated; brains were removed, iced, and blocked for slicing. The blocked tissue was cut into 300 μm thick slices with a Microslicer (Dosaka EM), while being bathed in oxygenated Kreb's solution composed of (in mM): 126 NaCl, 2.5 KCl, 1.25 NaH_2PO_4, 1 $MgCl_2$, 2 $CaCl_2$, 26 $NaHCO_3$, and 10 glucose (310 ± 5 mOsm/L, pH 7.4; bubbled with 95%O_2 and 5%CO_2). The slices were incubated at room temperature for at least 1 h in oxygenated Kreb's solution containing 0.2 mM ascorbic acid and 4 mM lactic acid. The slice was transferred to a recording chamber mounted on an upright microscope (Carl Zeiss) and continuously perfused with oxygenated Kreb's solution. Temperature of the bath solution in the recording chamber was adjusted to 30°C. Whole-cell recordings were performed using an EPC-9 double amplifier (HEKA Elektronik) controlled with a Macintosh computer running Pulse software (HEKA Elektronik). Electrodes were pulled from glass capillary tubes (Narishige) and fire-polished. The recording pipettes were filled with a solution containing (in mM): 130 potassium methylsulfate, 0.5 EGTA, 2 $MgCl_2$, 2 Na_2ATP, 0.2 GTP, 20 HEPES, 0.1 leupeptin and 0.75% biocytin (pH 7.2, 290 ± 5 mOsm/L) and had resistances of 5–7 MΩ in the bath. In experiments using glutamate stimulation, 1 mM sodium glutamate were dissolved in Kreb's solution and filled into the same pipettes as the one for whole-cell recordings. To avoid cells with their axons cut a lot by slicing, we did not stimulate cells located at the surface of slices. Stimulated L2/3 cells were typically located 20–50 μm deep from the slice surface. We positioned the pipette filled with glutamate within 10 μm distance from the soma aimed to trigger the spike and added air pressure (5–10 psi, 50 ms duration) to eject the glutamate solution onto the target cell. To calculate the connection and common input probabilities using glutamate stimulation, we discarded L5 pyramidal cells without any EPSC induction and L5 pairs without any simultaneous EPSC induction, respectively. This means that the probabilities used did not include zero. Even if we included cases with no common inputs, but EPSCs in both L5 cells, we obtained similar results (supplemental Fig. 1, available at www.jneurosci.org as supplemental material). For the analysis of firing patterns of cells, recordings were obtained immediately (3 min maximum) after membrane rupture. To quantify the voltage sag in response to negative current pulse injections, we measured the voltage difference between the negative peak and the end of membrane potentials to the current pulse (amplitude, −500pA; duration, 1 s) applied from resting membrane potentials adjusted to −60 mV by DC current injections. Data are represented as mean ± SD and statistical difference between samples was tested using ANOVA. Significance was accepted when $p < 0.05$.

Retrograde labeling. To identify pyramidal subtypes, retrograde fluorescent tracer, Alexa Fluor 555-conjugated cholera toxin subunit B (Invitrogen) or rhodamine-labeled latex microspheres (Lumafluor), was injected into contralateral striatum, ipsilateral pontine nuclei, or contralateral frontal cortex using similar procedures described previously (Morishima and Kawaguchi, 2006). Animals were anesthetized with ketamine (40 mg/kg, i.m.) and xylazine (4 mg/kg, i.m.). After injection of fluorescent retrograde tracer, animals were fed for 2–3 d as a recovery period before slice experiments.

Histology. Slices containing cells intracellularly labeled with biocytin were fixed with a solution containing 4% paraformaldehyde, 1.25% glutaraldehyde, and 0.2% picric acid in PB. After rinsing in PB, slices were treated with PB containing 1% H_2O_2 for 20 min and were resectioned at a thickness of 50 μm. Sections were then incubated with avidin-biotin-horseradish peroxidase complex (1%; Vector Laboratories) in 0.05M Tris-buffered saline (TBS) with 0.05% Triton X overnight at 4°C. After washing in TBS, sections were reacted with a mixture of 3,3′-diaminobenzidine tetrahydrochloride (0.02%), nickel ammonium sulfate (0.3%) and H_2O_2 (0.001%) in TBS. Then, sections were postfixed in 1% OsO_4 in PB containing 7% glucose, rinsed in PB, dehydrated in graded ethanol series, mounted on glass slides, and coverslipped with Epon for observation with a light microscope. Neurolucida system (MicroBrightField) was used for a reconstruction of stained cell.

Results

Three firing subtypes of L5 pyramidal cells

L5 pyramidal cells are heterogeneous in their morphological and physiological properties, and project to multiple subcortical areas. To examine their physiological properties, we obtained whole-cell recordings from frontal L5 pyramidal cells. L5 pyramidal cells did not fire spontaneously at the resting membrane potential. During depolarizing current pulse injections, L5 pyramidal cells displayed distinct patterns of spike discharge that were used to classify L5 pyramidal cells into three subtypes (Fig. 1*A*). One class of L5 cell reduced firing frequencies of spike trains during current pulse injection [fast spike frequency adaptation (FA) type (Fig. 1*A*, right traces)], whereas the other cells showed repetitive spike discharges with relatively steady spike frequencies during the current pulse injection [slow spike frequency adaptation (SA) type (Fig. 1*A*, left traces)]. In cells fired repetitively during the entire period of the current pulse, some of them showed initial burst (doublet) spikes at the beginning of the spike trains [Fig. 1*A*, asterisk and inset; slow spike frequency adaptation with initial doublet firing (SA-d) type; middle traces]. From firing frequencies (f) calculated from the first, second, seventh, and shortest interspike intervals [f1, f2, and f7 (Fig. 1*C*, inset) during the current pulse injection (amplitude, 500pA; duration, 1 s)] in individual cells, we obtained the burst (f1/f2), the adaptation index (f7/f2), and the maximum frequency. Shown in Figure 1*B* is the relation between the maximum firing frequency and the adaptation index obtained for L5 pyramidal cells including all cells in which we examined the specificity of connections from L2/3 pyramidal cells. Thus, we quantitatively identified three non-overlapped firing subtypes of L5 pyramidal cell. The burst index of SA-d type cells was significantly higher value than those found in SA and FA type cells (Fig. 1*C*, left histogram) (1.59 ± 0.46, 7.42 ± 3.36, and 2.14 ± 0.66, for SA, SA-d, and FA type, respectively, $n = 150$ for each subtype, $p < 0.01$). The adaptation index of FA type cells was lower than for those of other types (Fig. 1*C*, right histogram) (0.89 ± 0.16, 0.83 ± 0.28, and 0.1 ± 0.12, for SA, SA-d, and FA type, respectively, $n = 150$ for each subtype, $p < 0.01$). All three subtypes of L5 pyramidal cell showed a prominent voltage sag, a sign of the activation of h-current (McCormick and Pape, 1990), in response to negative current pulse injections (Fig. 1*A*, bottom traces). However, among three pyramidal subtypes, FA type cells had significantly larger voltage sag (Table 1) ($p < 0.01$). We also found significant differences in other physiological parameters including resting membrane potentials, input resistance, mean spike frequencies calculated with the exception of f1 (average frequency), and maximum spike frequency between L5 pyramidal subtypes (Table 1).

Pyramidal cells with poorly developed apical tufts were found to be FA type cells, whereas those with dense tufts were physiologically classified as SA or SA-d type cells (Fig. 1*A*). In the frontal cortex, L5 pyramidal cells have been divided into two major projection types: those innervating both sides of the striatum: crossed corticostriatal (CCS) cells, and corticopontine (CPn)

cells that extend their axons to pontine nuclei (Cowan and Wilson, 1994; Levesque et al., 1996; Reiner et al., 2003; Morishima and Kawaguchi, 2006). CCS cells often show the slender sparsely tufted dendritic morphologies whereas CPn cells generally have thick dendritic tufts (Morishima and Kawaguchi, 2006). Correlation between morphologies and projection targets has been also described in the motor cortex (Gao and Zheng, 2004; Hattox and Nelson, 2007). Here we examined the correlation between firing patterns and projection subtypes in the frontal cortex. Recordings from L5 pyramidal cells identified by retrograde fluorescent tracer revealed that most CCS cells (30 of 34 cells) were FA type cells, whereas very few CCS cells showed SA type firing pattern ($n = 4$ of 34). In contrast, CPn cells exhibited SA or SA-d type firing ($n = 29$ and 10 of 39, respectively), but no FA type cells were found (Fig. 1*D*). To further examine the relationship between firing subtypes and their projection sites, we obtained recordings from L5 commissural pyramidal cells projecting to the contralateral frontal cortex (COM cells). It has been shown that a subset of CCS cells projects to the contralateral cortex (Wilson, 1987). Unlike CCS and CPn cells, COM cells showed all three types of firing patterns ($n = 13$, 9, and 16 of 38 cells for SA, SA-d, and FA, respectively) (Fig. 1*D*), suggesting that COM cells contained both CCS and other type of L5 pyramidal cells. These results suggest that the subcortical projection subtype of frontal pyramidal cells is correlated with the intrinsic firing subtype, but also that a firing subtype includes more than one projection subtype. The burst and adaptation indices of the three subtypes of labeled cells were similar with those calculated for nonlabeled L5 pyramidal cells (retrogradely labeled cells: f1/f2, 1.46 ± 0.42 for SA, 6.82 ± 2.74 for SA-d, and 2.07 ± 0.73 for FA; f7/f2, 0.91 ± 0.19 for SA, 0.88 ± 0.31 for SA-d, and 0.074 ± 0.13 for FA). Similar correlations between firing properties and subcortical projection targets have been reported in the mouse motor cortex (Hattox and Nelson, 2007).

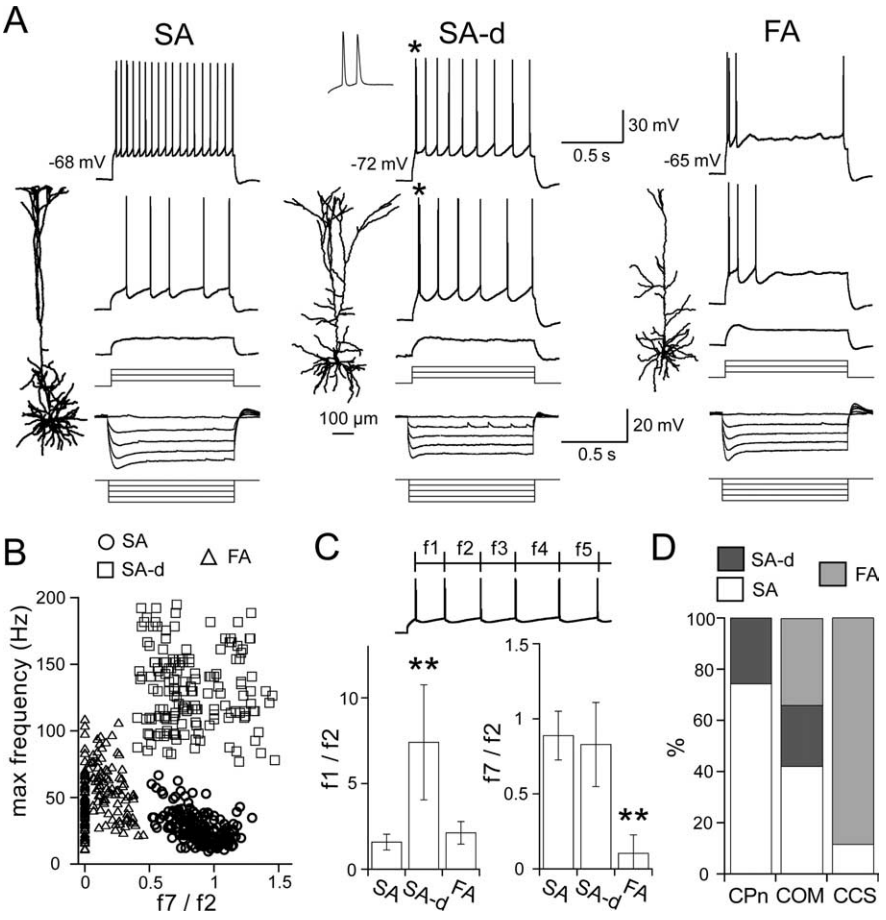

Figure 1. Three firing subtypes of L5 pyramidal cells and their correlation with projection targets. ***A***, Dendritic reconstructions and voltage responses to current injections in SA, SA-d, and FA type L5 pyramidal cells (pulse duration, 1 s; amplitude, from −400 to +500 pA in 100pA steps). Asterisk indicates initial doublet spikes. Inset in SA-d, initial doublet (*) at an expanded time scale and reduced voltage scale. ***B***, Distribution of the relation between maximum spike frequency and the adaptation index (f7/f2) obtained from spike trains generated by current injection (500pA) in three L5 pyramidal subtypes ($n = 183$, 161, and 180, for SA, SA-d, and FA type cell, respectively). Spike frequency (f) was calculated from each interspike interval (see inset in ***C***). Note that three clusters are readily identified by the two firing parameters. ***C***, Comparisons of f1/f2 (burst index) and f7/f2 (adaptation index) between SA, SA-d, and FA type pyramidal subtypes ($n = 150$, respectively). Data are means ± SD; $^{**}p < 0.01$. ***D***, Proportion of firing subtypes among CPn ($n = 39$), COM ($n = 38$) and CCS ($n = 39$) cells identified by retrograde fluorescent tracers.

Detection of synaptic inputs by glutamate puff stimulation

Focal glutamate stimulation to induce action potentials in the cells located restricted area has been widely used to analyze synaptic connections in cortical networks (Schubert et al., 2003; Shepherd and Svoboda, 2005; Shepherd et al., 2005; Yoshimura and Callaway, 2005; Yoshimura et al., 2005). Focal glutamate stimulation allows us to test functional connections to a single recording cell from a large number of cells, individually. To investigate the specificity of synaptic connections from L2/3 to L5 pyramidal cells, we also took advantage of the glutamate stimulation to induce action potentials in L2/3 pyramidal cells. Glutamate was focally applied through the glass pipette placed nearby the soma of L2/3 pyramidal cell aimed to trigger the spike.

Whole-cell or cell-attached recordings were obtained from L2/3 pyramidal cells to examine whether this method reliably induces spikes in the cell (Fig. 2*A*). Although L2/3 pyramidal cells do not fire spontaneously, observed at either cell-attached or whole-cell mode, in the slice preparation, a focal puff of glutamate (1 mM, 50 ms; 5–10 psi) reliably evoked a single spike in L2/3 pyramidal cells when the puff pipette was placed very close to the soma (Fig. 2*A*, upper trace). The latency of spike measured from the glutamate puff onset to the spike peak was 60.1 ± 20.6 ms ($n = 20$). The SD of delays for individual stimulations, representing the variability of the spike timing, was 8.4 ± 4.1 ms. Spikes disappeared when the pipette was moved slightly away from the soma (Fig. 2*A*, lower trace). Glutamate-induced spikes were completely abolished when puff pipettes were positioned 9.8 ± 2.7 μm away from the soma (Fig. 2*B*). To examine the single cell stimulation selectivity by glutamate puff, we obtained recordings from two close neighboring L2/3 pyramidal cells with whole-cell or cell-attached mode, while applying glutamate to either of the two cells. We found that glutamate-puff application evoked a single spike only in one cell that we selected, but not in the other

Table 1. Basic intrinsic membrane properties and EPSCs to L5 pyramidal subtypes

cell type	Vrest (mV)	Ri (MΩ)	Max frequency (/s)	Average frequency (/s)	Vsag (mV)	EPSCs from L2/3 amplitude (pA)	EPSCs from L2/3 rise time (ms)	EPSCs from L2/3 decay (ms)	EPSCs from L5 amplitude (pA)	EPSCs from L5 rise time (ms)	EPSCs from L5 decay (ms)
SA	-68.4 ± 3.4	72.3 ± 19.7	26.9 ± 11.4	15.1 ± 7.4	4.8 ± 1.6	10.7 ± 4.4	3.0 ± 0.9	23.2 ± 7.2	11.3 ± 8.3	2.4 ± 0.5	18.8 ± 8.1
SA-d	-70.0 ± 3.2	81.2 ± 19.7	131.1 ± 28.7	15.5 ± 4.0	4.6 ± 1.2	11.9 ± 4.7	2.6 ± 0.5	22.2 ± 6.3	14.4 ± 14.4	2.7 ± 0.9	20.7 ± 6.7
FA	-67.7 ± 4.8	103.2 ± 29.9	51.9 ± 20.7	13.5 ± 4.1	6.1 ± 1.6	13.2 ± 6.6	3.0 ± 0.9	23.0 ± 5.2	11.9 ± 5.2	2.2 ± 0.7	21.1 ± 4.8
	SA, FA ** SA-d	FA ** SA-d ** SA	SA-d ** FA ** SA	SA, SA-d * ** FA	FA ** SA, SA-d						
				*<0.01, *<0.05		n = 11 for SA n = 10 for SA-d n = 10 for FA			n = 25 for SA n = 18 for SA-d n = 12 for FA		
	n = 150 for individual types										

Values are given as mean ± SD. Max frequency, Maximum spike frequency; Ri, input resistance; Vrest, voltage rest; Vsag, voltage sag.

cell (Fig. 2*C*) ($n = 12$ cell-pairs). Thus, glutamate puff stimulation can selectively induce a single spike in individual L2/3 pyramidal cells.

To examine whether L2/3 pyramidal cell stimulation by glutamate puff can evoke EPSCs in L5 pyramidal cells, we obtained whole-cell recordings from L5 pyramidal cells while puff-applying glutamate to L2/3 pyramidal cells. If a stimulated L2/3 pyramidal cell has synaptic connections with a recorded L5 pyramidal cell, we would detect EPSCs at relatively constant timings after the glutamate puff because of stable spike triggering in the L2/3 pyramidal cell by the stimulation (Fig. 2). We applied glutamate to individual L2/3 pyramidal cells at least 10 times at every 3 s. As expected, EPSCs were evoked at relatively constant latencies among the trials by L2/3 pyramidal cell stimulation (Fig. 2*D*). After EPSC detection by glutamate puff, we obtained whole-cell recordings from the glutamate-stimulated L2/3 pyramidal cell to confirm monosynaptic connections to the recorded L5 pyramidal cell (Fig. 2*E*). We confirmed monosynaptic connections in nearly 90% of connections detected by glutamate puff (30 of 34 pairs). We did not obtain reciprocal connections from L5 to L2/3 pyramidal cells in these cell pairs. Some glutamate puffs induced long lasting inward currents clearly distinguished from EPSCs. Those were probably induced by direct dendritic stimulation of recorded L5 pyramidal cells, because the amplitude and the duration of inward currents were dependent on the intensity and the duration of the puff stimulation (data not shown). These results indicate that focal glutamate stimulation allows testing for monosynaptic connections between cortical cells.

Connection properties from L2/3 to L5 pyramidal cells

By combining glutamate stimulation to L2/3 pyramidal cells and whole-cell recordings, we examined the synaptic connection properties from L2/3 to L5 pyramidal subtypes. First, the connection probability from L2/3 to L5 pyramidal cells was compared among the physiologically identified L5 pyramidal cell subtypes. The connection probability from L2/3 to individual L5 pyramidal cells was calculated from the number of stimulated L2/3 cells that induced synaptic inputs and the total number of L2/3 cells stimulated with glutamate during the recording. Stimulated L2/3 cell number for each L5 pyramidal cells was 23.7 ± 7.8 (ranged from 15 to 50). The connection probability from L2/3 cells to L5 SA and SA-d cells was 0.191 ± 0.093 and 0.196 ± 0.092, respectively ($n = 117$ and 98 for SA and SA-d). FA type L5 pyramidal cells, however, received synaptic inputs from L2/3 pyramidal cells with a lower connection probability than other L5 subtypes ($p = 0.105 \pm 0.062$, $n = 92$, $p < 0.01$) (Fig. 2*F*).

To examine for functional differences in the synaptic connections from L2/3 to L5 pyramidal subtypes, we compared the kinetics and frequency characteristics of unitary EPSCs obtained from cell pairs of L2/3 and L5 pyramidal cells by dual whole-cell recordings. The amplitude of EPSCs evoked by a single spike in the L2/3 cell varied between cell pairs. No significant difference was found in the mean amplitude, rise time, and decay of EPSCs between L5 pyramidal subtypes (Table 1). The paired-pulse ratio of the second to first EPSCs amplitudes was calculated from responses evoked by presynaptic spikes delivered at 10 Hz. To avoid the error of analysis (Kim and Alger, 2001), we calculated the ratio as the mean amplitude of the second response divided by that of the first. Both paired-pulse facilitation and depression were observed in all L5 pyramidal subtypes. Shown in Figure 3*A* is a relation between the mean amplitude and the paired-pulse ratio of EPSCs. The paired-pulse ratio depended on the EPSCs amplitude; that is, paired-pulse depression was found more often in connections generating large EPSCs whereas paired-pulse facilitation was observed in connections generating small EPSCs. A similar relationship between the amplitude of EPSCs and paired-pulse ratio has been reported in the hippocampus (Debanne et al., 1996).

For comparison, we investigated the synaptic connection property between L5 pyramidal cells by dual whole-cell recordings. We tested connections between L5 pyramidal cells in 493 cell pairs and found that the connection probabilities from presynaptic SA cells were 0.063 (to other SA, 12/107 cell-pairs), 0.04 (to SA-d cells, 5/125 cell-pairs), and 0.049 (to FA cells, 3/61 cell-pairs). For presynaptic SA-d cells, connection probabilities were 0.056 (to SA, 7/125 cell-pairs), 0.081 (to other SA-d, 9/62 cell-pairs), and 0.032 (to FA, 2/62 cell-pairs). Connection probabilities from presynaptic FA cells were 0.1 (to SA, 6/60 cell-pairs), 0.065 (to SA-d, 4/62 cell-pairs), and 0.053 (to FA, 8/76 cell-pairs). For the same subtype cell pairs, we considered the direction and the reciprocity of connections. The connection probabilities from FA type to SA or SA-d type tend to be higher than the other direction (i.e., from SA or SA-d to FA type cell). Reciprocal connections were found only in SA/SA and SA-d/SA-d type cell pairs. We note that these connection probabilities were obtained from cell-pairs of L5 pyramidal subtypes classified by firing patterns. It has been shown that connections between L5 pyramidal projection subtypes are direction selective (Morishima and Kawaguchi,

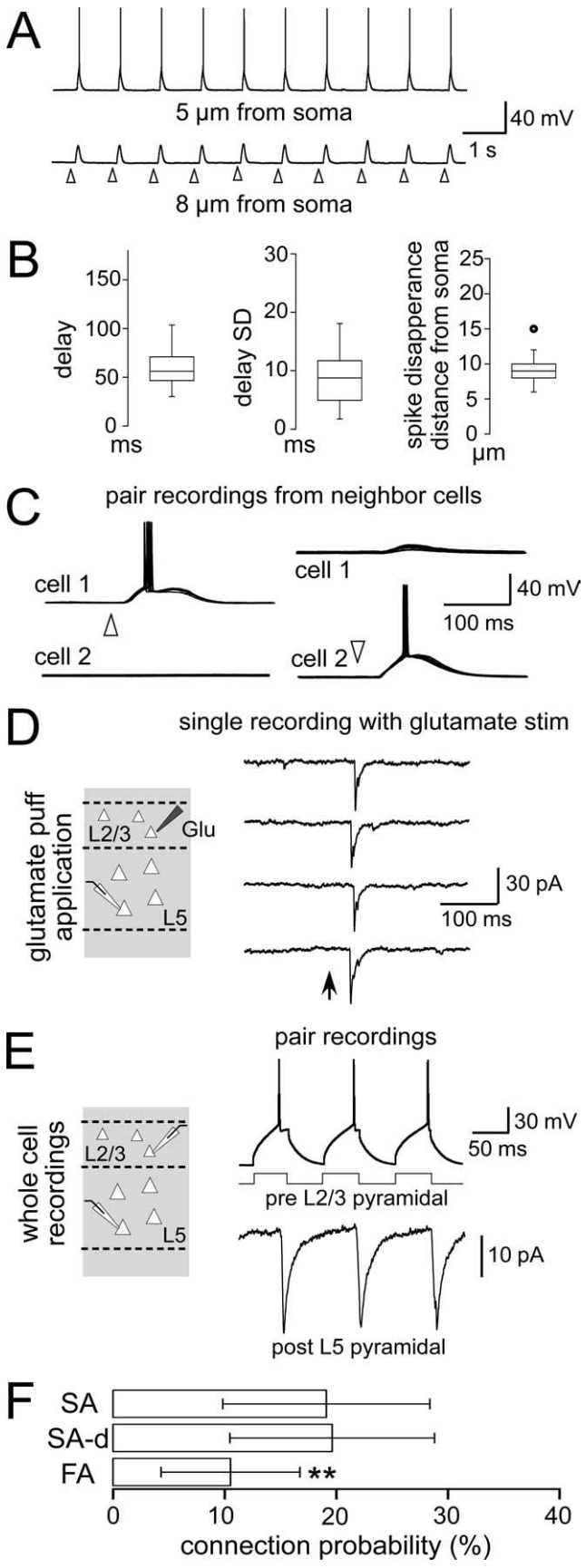

Figure 2. EPSC induction in L5 cells by glutamate puff stimulation to L2/3 pyramidal cells. ***A***, Responses to glutamate puff applications in a L2/3 pyramidal cell. The puff pipette was positioned to 5 μm (top trace) or 8 μm (bottom trace) away from the recorded soma. Arrowheads denote timing of glutamate puff-application (duration, 50 ms). ***B***, Box plot summaries of data for means and SDs of spike induction latencies from the puff onset to the spike peak calculated for individual cells, and the minimum distances from the soma to the pipette that completely eliminate spike production ($n = 20$ cells; 12 cells in whole-cell and 8 cells in cell-attached modes). ***C***, Recordings from two close neighboring L2/3 pyramidal cells while applying glutamate to either of the two cells. Arrowhead indicates the timing of glutamate puff-application. Ten traces were superimposed. ***D***, Synaptic inputs were detected in L5 pyramidal cells by glutamate puff stimulation to L2/3 pyramidal cells. Arrow indicates glutamate puff onset. ***E***, Verification of EPSC induction by glutamate puff by following dual whole-cell recordings from the stimulated L2/3 cell in addition to the L5 cell. Monosynaptic connections were confirmed in 30 of 34 cases. ***F***, Interlaminar connection probabilities from L2/3 to L5 pyramidal subtypes ($n = 117$, 98, and 92 for SA, SA-d, and FA type). Data are presented as means ± SD; $^{**}p < 0.01$.

2006). As shown in Figure 1*D*, COM cells exhibited all three firing subtypes, indicating that one firing subtype includes several projection subtypes of L5 pyramidal cells. The kinetics of unitary EPSCs to L5 pyramidal subtypes was independent of postsynaptic cell subtypes (Table 1). Similarly, no significant differences were found in EPSCs kinetics between L2/3 to L5 and L5 to L5 connections. We also examined short-term synaptic plasticity for EPSCs generated from connections between L5 pyramidal cells, and observed both paired-pulse depression and facilitation in all subtypes. Again, a similar relationship between the paired-pulse ratio and EPSCs amplitude in L2/3 to L5 connections was observed in connections between L5 pyramidal cells (Fig. 3*B*). These results suggest that synaptic properties of connections from L2/3 to L5 pyramidal cells are not distinct from those from L5 to L5 pyramidal cells.

Next, we investigated depth distribution of presynaptic L2/3 cells to L5 pyramidal cells. The somatic position of presynaptic L2/3 and postsynaptic L5 cells was measured vertically from the border between layer 1 and layer 2. Shown in Figure 4 is the relation between depth location of EPSC induced L2/3 and postsynaptic L5 cells in glutamate puff stimulation experiments. Both SA and SA-d type L5 pyramidal cells received synaptic inputs from the entire depth of L2/3, whereas EPSC induction in FA type L5 cells was dependent on the location of their somata. Stimulation of L2/3 cells located in the upper part of L2/3 tended to induce EPSCs in FA type cells localized to the upper areas of L5. In contrast, FA type cells located in the lower part of L5 received inputs from lower L2/3 cells. Thus, interlaminar depth correlation between presynaptic and postsynaptic pyramidal cells was found in FA type cells ($p < 0.01$). Together, the subtype differences in connection probability and interlaminar connection topography suggest the existence of multiple different synaptic pathways from L2/3 to L5 cells.

Divergence selectivity from L2/3 to L5 pyramidal subtypes

Pyramidal cells in one layer innervate cells in other layers selectively according to connectivity of the recipient or sender pyramidal cells (Shepherd and Svoboda, 2005; Song et al., 2005; Yoshimura et al., 2005; Kampa et al., 2006). The connection probability from a single cell to two postsynaptic cells in another layer is higher when two recipient cells have connections with each other, suggesting the existence of segregated cortical pathways dependent on connectivity of the recipient layer (Yoshimura et al., 2005; Kampa et al., 2006). However, it remains unknown whether there exist functional channels dependent on pyramidal subtypes in the recipient layer.

To address this, we obtained dual whole-cell recordings from pairs of closely located L5 pyramidal cells with combination of same or different subtypes, while stimulating L2/3 pyramidal cells with glutamate (Fig. 5*A*). The distances between the somata of L5

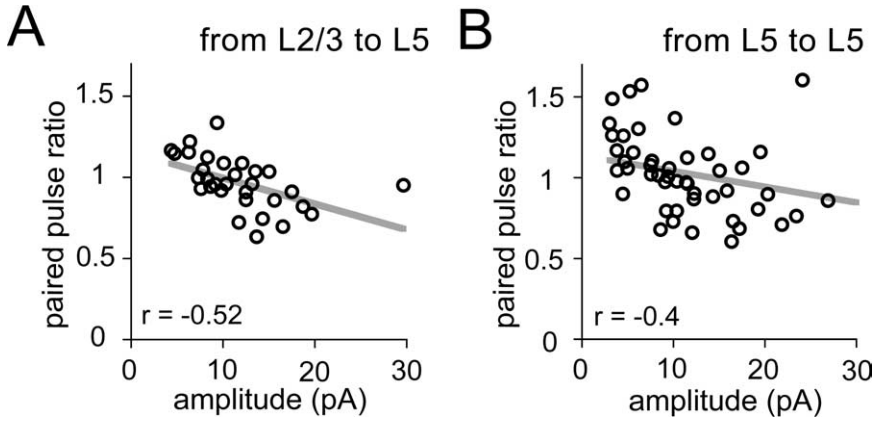

Figure 3. Synaptic frequency characteristics depend on the EPSC amplitude. ***A***, ***B***, Relationship between the mean EPSC amplitude and the paired pulse ratio in L2/3 to L5 connections ($n = 31$) in ***A*** and L5 to L5 connections ($n = 49$) in ***B***. Ten to twenty recordings of EPSCs evoked by two successive presynaptic spikes (10 Hz) were averaged in individual connections. The paired pulse ratio was calculated by the mean of the second response divided by the mean of the first EPSC amplitude.

cell pairs were typically within 50 μm in both the horizontal and vertical directions. If both L5 neurons receive synaptic inputs from the same L2/3 pyramidal cell, synchronous EPSCs should be observed in both L5 cells by glutamate stimulation (Shepherd and Svoboda, 2005; Yoshimura and Callaway, 2005; Yoshimura et al., 2005). After determining the firing types and synaptic connectivity between two L5 pyramidal cells (Fig. 5*B*), we examined common input probability that two L5 cells receives synchronous inputs from L2/3 cells. In some L5 cell pairs, glutamate stimulation induced simultaneous EPSCs in both L5 cells. These synchronous EPSCs were observed stably in both cells at relatively constant latencies in multiple stimulus trials, suggesting excitatory inputs from the same presynaptic cell (Fig. 5*C*, right traces). Glutamate stimulation of some other L2/3 cells induced EPSCs in either of the two L5 cells (Fig. 5*C*, left traces). We calculated the common input probability for each pair of L5 cells by dividing the number of glutamate-stimulated L2/3 cells that induced simultaneous EPSCs in both L5 cells by total number of glutamate-stimulated L2/3 cells (see supplemental information, available at www.jneurosci.org as supplemental material).

The connection probabilities from L2/3 to L5 pyramidal cells depended on the subtypes of postsynaptic L5 pyramidal cells (Figs. 2*F*; 5*D*, upper box). To compare the common input probability among L5 pyramidal subtypes, we normalized common input probabilities for different postsynaptic cell types relative to the probabilities expected for nonselective innervation to two L5 cells (Fig. 5*D*, lower box). The hypothetical common input probability in nonselective cases was calculated by $p_1 \times p_2$. The p_1 and p_2 are the probabilities that L5 cell receives inputs from a given L2/3 cells, taking different values determined experimentally for the different L5 subtypes (i.e., $p = 0.191$, 0.197, and 0.105, for SA, SA-d, and FA cells, respectively).

To distinguish between the effects of subtype combination and intralaminar connectivity between two L5 cells, we first compared the common input probability between unconnected L5 cell pairs, using the ratio of the observed probability and the expected probability assuming nonselective innervations (Fig. 5*E*). The relative probability was close to one in cell pairs of different L5 pyramidal subtypes. However, when both L5 cells were of the same subtype, the common input probability ratio was significantly higher than those in the different subtype pairs (2.57 ± 0.85, 2.5 ± 0.54, and 2.79 ± 0.74 for SA/SA, SA-d/SA-d, and FA/FA cell pairs, respectively). These results suggest that L2/3 pyramidal cells innervate L5 pyramidal cells selectively depending on the subtype of the L5 target neurons.

We, next, examined whether the synaptic connectivity between L5 cells influences the common input probability from L2/3. We compared the common input probabilities between connected and unconnected cell pairs separately in pairs consisting of cells of the same (homo) and different (hetero) L5 subtypes. For connected cell pairs, we adopted L5 cell pairs with both one way and reciprocally connections. Connections from L2/3 to L5 pyramidal cells were highly selective when L5 cells were of the same physiological subtype and had connections between them (Fig. 6*A*). The common input probability ratio was 3.76 ± 0.88 for connected pairs of the same subtype, higher than one for unconnected cell pairs of the same subtype (2.59 ± 0.68, $p < 0.01$). However, in pairs of different L5 subtypes, the common input probability did not depend on connectivity between L5 cells (1.32 ± 0.34 for connected pairs, 1.38 ± 0.33 for unconnected pairs, $p = 0.556$). Even if we included cases with no common inputs, but EPSCs in both L5 cells, common input probabilities between two L5 pyramidal cells showed similar specificity dependent on their subtype combination and connectivity (supplemental Fig. 1, available at www.jneurosci.org as supplemental material).

Discussion

In this study, we examined the specificity of excitatory connections from L2/3 to L5 pyramidal subtypes, classified by their firing properties. We found that L5 pyramidal cells received synaptic inputs from L2/3 pyramidal cells with different connection probability and intralaminar location of presynaptic and postsynaptic cell soma, in a subtype-dependent manner. Moreover, we showed that L5 pyramidal cells received common excitatory inputs from L2/3 pyramidal cells dependent on firing subtypes of L5 cells and synaptic connectivity between them; higher probabilities to L5 cell pairs of the same subtype than the different one; and highly selective to connected L5 cell pairs of same subtype, but not of different firing patterns (Fig. 6*B*). Our results suggest that excitatory connections from L2/3 to L5 pyramidal cells form subnetworks dependent on L5 pyramidal subtypes.

L5 pyramidal cells project to various subcortical structures (Wise and Jones, 1977). Recent studies have found correlations between the dendritic morphologies of L5 pyramidal cells and their extracortical axonal targets (Reiner et al., 2003; Gao and Zheng, 2004; Morishima and Kawaguchi, 2006; Hattox and Nelson, 2007). Furthermore, a group of L5 pyramidal cells projecting to the same extracortical target share common electrophysiological properties (Hattox and Nelson, 2007). Here, we have quantitatively confirmed the relationship between firing patterns of frontal L5 pyramidal cells and their subcortical projection patterns to contralateral striatum or ipsilateral pontine nuclei. These observations suggest that the cortical output to subcortical areas is conveyed by target-specific groups of pyramidal cells with distinct morphological and electrophysiological characteristics. Frontal L5 pyramidal cells projecting to contralateral cortex, however, exhibited all three firing subtypes (Fig. 1*D*), suggesting that one firing subtype contains multiple projection subtypes. In

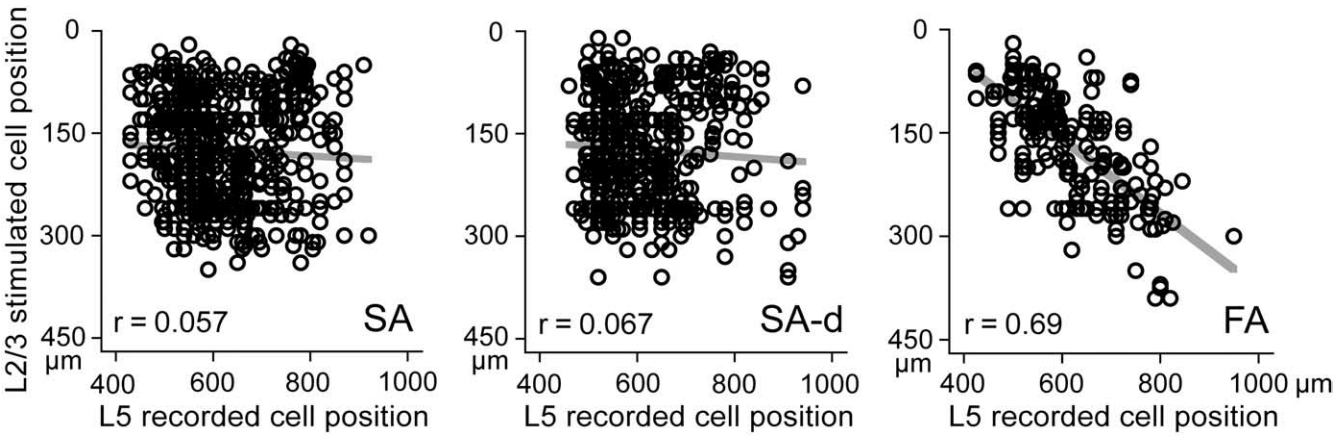

Figure 4. Interlaminar connection maps to L5 pyramidal subtypes. Relationship between somatic locations of presynaptic L2/3 cells and of postsynaptic L5 pyramidal cells varied among L5 firing subtypes. Cell positions were measured as the vertical distance from the L1 and L2/3 border. Regression lines indicate the interlaminar topographic connections to FA type L5 cells, but not to SA or SA-d cells.

the parietal associative and visual cortical area, L5 pyramidal cells projecting to the superior colliculus or contralateral cortex show similar firing properties (Christophe et al., 2005). Together, correlation between the firing properties and axonal projections of pyramidal cell differs according to cortical areas and extracortical targets.

We classified firing patterns of pyramidal cells to three types based on initial burst firing and the spike frequency adaptation during current pulse injection. Spike discharge patterns to depolarizing current pulses have been studied for a long time. In a way similar to ours, several studies have identified three or more groups of L5 pyramidal cells by *in vitro* or *in vivo* recordings from various cortical areas and species (Connors et al., 1982; Nuñez et al., 1993; Schwindt et al., 1997; Dégenètais et al., 2002; Schubert et al., 2006; Chang and Luebke, 2007). It has been shown that burst firing of pyramidal cells is influenced by many factors, such as intracellular and extracellular Ca^{2+} concentration (Friedman and Gutnick, 1989; Su et al., 2001; Golomb et al., 2006) and prolonged exposure to anesthesia (Christophe et al., 2005). The SA-d type cells, described here, which fired an initial doublet followed by trains of single spikes, may correspond to intrinsically bursting (IB) cells that have been described as fired with an initial burst of 3 and more spikes (Connors et al., 1982; Agmon and Connors, 1992; Nuñez et al., 1993; Gray and McCormick, 1996). However, we did not find the morphological or axonal target differences between SA and SA-d type cells, as has been described between regular spiking and IB pyramidal cells in the somatosensory cortex (Schubert et al., 2006). Regardless, the connection specificity dependent on SA and SA-d types suggests that these cell types play distinct functional roles in cortical circuits.

We found the connection probability from L2/3 to FA type L5 cells was lower than the probability of connections onto SA or SA-d cells. This finding corresponds well with a previous report that L5 pyramidal cells with thick tufted apical dendrites (as found here in SA and SA-d cells) receive more frequent inputs from L2/3 pyramidal cells than those with slender apical dendrites (Thomson and Bannister, 1998). In the barrel cortex, however, both types of L5 pyramidal cells received inputs from L2/3 pyramidal cells with similar connection probabilities (Schubert et al., 2001), suggesting the differences between cortical areas in connection probabilities from L2/3 to L5 pyramidal subtypes. Although L5 pyramidal cells make axonal contacts mainly on basal dendrites of other L5 pyramidal cells, L2/3 pyramidal cells are likely to innervate apical dendrites of L5 pyramidal cells (Letzkus et al., 2006; Morishima and Kawaguchi, 2006; Sjöström and Häusser, 2006). The differences in apical dendritic arborization between pyramidal subtypes (Morishima and Kawaguchi, 2006), may contribute to differences in connection probability from L2/3 to L5 pyramidal subtypes. In addition, FA type cells received excitatory inputs from L2/3 cells in a topographic manner, depending on the depth of their soma in the layer. Given that a similar relationship was not seen in SA or SA-d cells, it is unlikely that this result is reflective of distance-dependent changes in connection probability, but rather reflects the functional topographical relationship between different subsets of L2/3 and L5 FA cells. It has previously been shown that L5 pyramidal cells projecting to different subcortical targets distribute unevenly within the layer (Wise and Jones, 1977; Killackey et al., 1989; Reiner et al., 2003). Thus, different interlaminar excitatory sources dependent on L5 subtypes may form further specialized subnetworks for particular subcortical targets.

Regardless of differences in connection probabilities and presynaptic cell locations, we found no obvious differences in synaptic properties from L2/3 to L5 pyramidal subtypes and connections between L5 subtypes. Both paired-pulse facilitation and depression, reflecting release probabilities of presynaptic terminals (Debanne et al., 1996), were found in all L5 subtypes. Optical quantal analysis revealed large variability of the release probability at synaptic boutons onto different postsynaptic pyramidal cells, but release probability of different boutons contacting to the same postsynaptic cells varied little (Koester and Johnston, 2005). Although frequency characteristics of synaptic transmission from pyramidal cell to inhibitory interneurons depend on the presynaptic pyramidal subtypes (Angulo et al., 2003), the frequency characteristics of connections between pyramidal cells may appear to be independent of subtype, and may rather be related to the plastic change of unitary connections.

The specificity of connections between cortical pyramidal cells has been elegantly investigated in studies using uncaged glutamate photostimulation and multiple recordings (Shepherd and Svoboda, 2005; Song et al., 2005; Yoshimura et al., 2005; Kampa

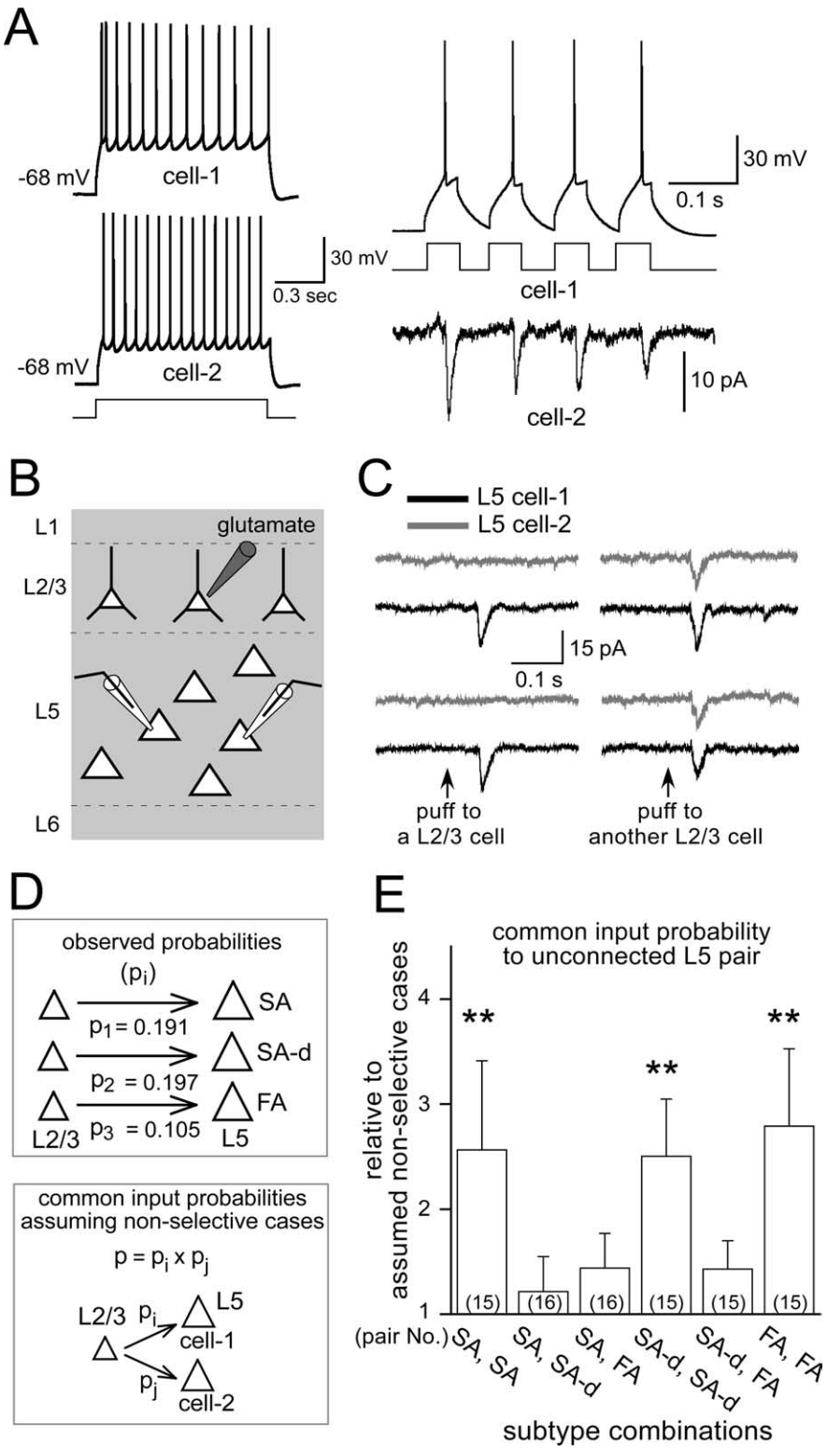

Figure 5. Divergent connection selectivity from L2/3 to L5 pyramidal subtypes. ***A***, Dual whole-cell recordings from L5 pyramidal cells. Left, Identification of firing subtypes (cell-1, SA-d; cell-2, SA). Right, EPSCs in cell-2 induced by cell-1 spikes. ***B***, Divergence connections to two L5 pyramidal subtypes tested by L2/3 cell stimulation by glutamate puff. ***C***, EPSC induction in two L5 cells. Left, EPSCs observed only in one cell; right, common inputs induced by L2/3 cell stimulation. ***D***, Top box, Observed connection probabilities from L2/3 to L5 pyramidal subtypes. Bottom box, Calculation of common input probabilities assuming nonselective innervations. ***E***, Probabilities that two L5 pyramidal cells share common inputs from a L2/3 cell in the case of unconnected L5 pairs, relative to those assuming nonselective cases. The common input probabilities were compared between subtype combinations of L5 pairs. Data are means ± SD; $^{**}p < 0.01$.

et al., 2006). However, these studies have not considered pyramidal cell heterogeneity in firing properties, morphologies, and subcortical targets. The glutamate puff stimulation used here can excite cells in a more restricted area (within 10 μm from the pipette tip) than the previous uncaging photostimulation (Dantzker and Callaway, 2000; Shepherd and Svoboda, 2005; Shepherd et al., 2005; Yoshimura and Callaway, 2005; Yoshimura et al., 2005). Using glutamate stimulation, we demonstrated divergence connectional selectivity from L2/3 to two L5 firing subtypes that are correlated with morphology and subcortical targeting. The common input probability obtained here might, however, have been overestimated, because of the limitation of the number of glutamate stimulated L2/3 cells. In addition, to calculate the common input probability, we adopted cell pairs in which we detected synchronous EPSCs during the recordings. These would reflect that the relative common input probabilities in all groups of L5 cell pairs showed >1. In the somatosensory cortex, L5 pyramidal cells receive common inputs from L2/3 pyramidal cells with higher probability than the assumed random cases when L5 pyramidal cells have connections with each other (Kampa et al., 2006). We investigated dependency of the common input probability from L2/3 to two L5 cells on the subtype combination and synaptic connectivity between two postsynaptic L5 cells. Common inputs from L2/3 to L5 cells were highly selective between connected cell pairs of the same subtype, but not different subtypes. Moreover, unconnected cell pairs of the same subtype received common inputs from L2/3 cells with higher probability than did cell pairs of different subtypes regardless of whether those cells were synaptically connected or not. Our results suggest that intralaminar neuron subtyping should be taken into account when analyzing interlaminar connections.

In the present study, we showed synaptic pathways from L2/3 to L5 pyramidal cells are differentiated according to L5 pyramidal firing subtypes. Firing properties of L5 pyramidal cells were correlated with particular extracortical targets (Fig. 1*D*) (Hattox and Nelson, 2007). Together, these observations suggest that the L2/3 to L5 excitatory pathway is composed of functionally segregated channels corresponding to projection systems to some extracortical targets. Interactions between different L2/3 to L5 excitatory subnetworks would be performed on connections between pyramidal cells in the same

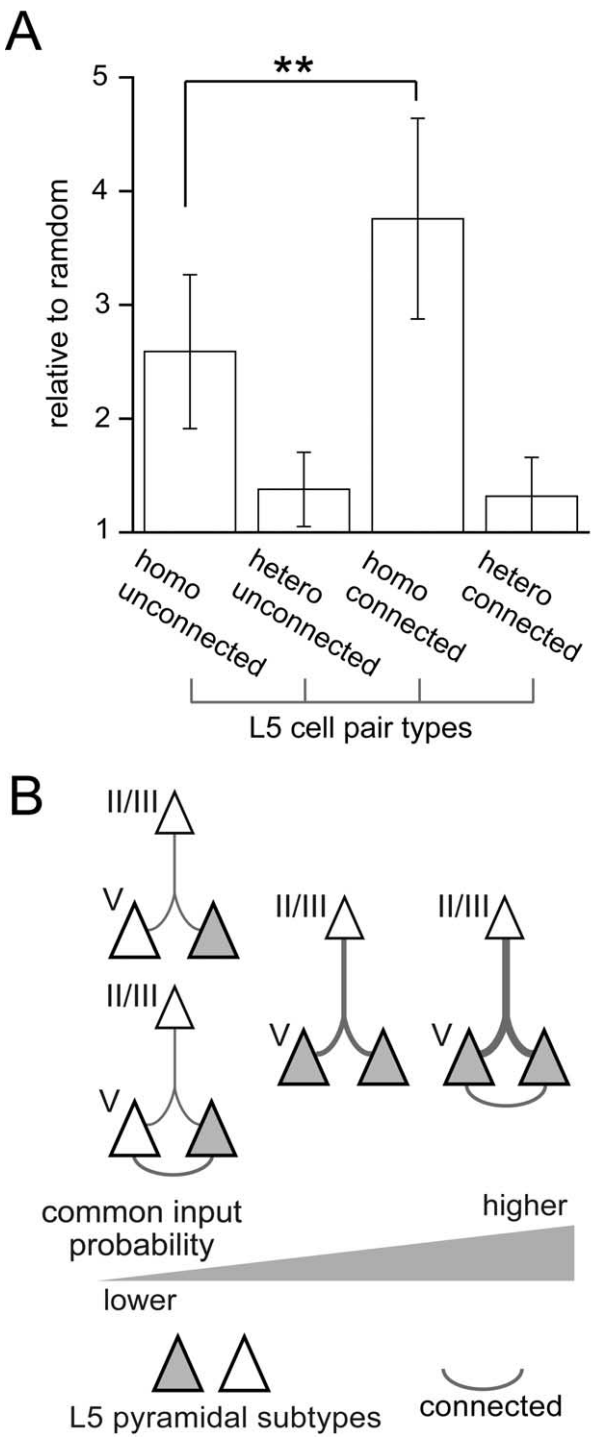

Figure 6. Effect of subtype homology and connectivity between L5 cells on connection selectivity from L2/3 pyramidal cells. ***A***, Common input probabilities to two L5 cells compared between the same (homo) and different (hetero) subtype pairs ($n = 45$ and 47 pairs, respectively), and between connected ($n = 15$) and unconnected pairs ($n = 15$). Data are means ± SD; $^{**}p < 0.01$. ***B***, Schematic diagram of interlaminar divergence selectivity from L2/3 to L5 pyramidal cells. Line thickness represents connection probabilities. Open and dark triangles indicate different pyramidal subtypes.

layer (L5 and L2/3). Moreover, the observation that connections between L5 projection subtypes are differentiated in a direction preference manner (Morishima and Kawaguchi, 2006) suggests the hierarchy among different L2/3 to L5 subnetworks for particular subcortical targets.

References

Agmon A, Connors BW (1992) Correlation between intrinsic firing patterns and thalamocortical synaptic responses of neurons in mouse barrel cortex. J Neurosci 12:319–329.

Angulo MC, Staiger JF, Rossier J, Audinat E (2003) Distinct local circuits between neocortical pyramidal cells and fast-spiking interneurons in young adult rats. J Neurophysiol 89:943–953.

Bureau I, von Saint Paul F, Svoboda K (2006) Interdigitated paralemniscal and lemniscal pathways in the mouse barrel cortex. PLoS Biol 4:e382.

Chagnac-Amitai Y, Luhmann HJ, Prince DA (1990) Burst generating and regular spiking layer 5 pyramidal neurons of rat neocortex have different morphological features. J Comp Neurol 296:598–613.

Chang YM, Luebke JI (2007) Electrophysiological diversity of layer 5 pyramidal cells in the prefrontal cortex of the rhesus monkey: in vitro slice studies. J Neurophysiol 98:2622–2632.

Cho RH, Segawa S, Mizuno A, Kaneko T (2004) Intracellularly labeled pyramidal neurons in the cortical areas projecting to the spinal cord. I. Electrophysiological properties of pyramidal neurons. Neurosci Res 50:381–394.

Christophe E, Doerflinger N, Lavery DJ, Molnár Z, Charpak S, Audinat E (2005) Two populations of layer V pyramidal cells of the mouse neocortex: development and sensitivity to anesthetics. J Neurophysiol 94:3357–3367.

Connors BW, Gutnick MJ, Prince DA (1982) Electrophysiological properties of neocortical neurons in vitro. J Neurophysiol 48:1302–1320.

Cowan RL, Wilson CJ (1994) Spontaneous firing patterns and axonal projections of single corticostriatal neurons in the rat medial agranular cortex. J Neurophysiol 71:17–32.

Dantzker JL, Callaway EM (2000) Laminar sources of synaptic input to cortical inhibitory interneurons and pyramidal neurons. Nat Neurosci 3:701–707.

Debanne D, Guérineau NC, Gähwiler BH, Thompson SM (1996) Paired-pulse facilitation and depression at unitary synapses in rat hippocampus: quantal fluctuation affects subsequent release. J Physiol 491:163–176.

DeFelipe J, Fariñas I (1992) The pyramidal neuron of the cerebral cortex: morphological and chemical characteristics of the synaptic inputs. Prog Neurobiol 39:563–607.

Dégenètais E, Thierry AM, Glowinski J, Gioanni Y (2002) Electrophysiological properties of pyramidal neurons in the rat prefrontal cortex: an in vivo intracellular recording study. Cereb Cortex 12:1–16.

Friedman A, Gutnick MJ (1989) Intracellular calcium and control of burst generation in neurons of guinea-pig neocortex in vitro. Eur J Neurosci 1:374–381.

Gao WJ, Zheng ZH (2004) Target-specific differences in somatodendritic morphology of layer V pyramidal neurons in rat motor cortex. J Comp Neurol 476:174–185.

Golomb D, Yue C, Yaari Y (2006) Contribution of persistent Na^+ current and M-type K^+ current to somatic bursting in CA1 pyramidal cells: combined experimental and modeling study. J Neurophysiol 96:1912–1926.

Gottlieb JP, Keller A (1997) Intrinsic circuitry and physiological properties of pyramidal neurons in rat barrel cortex. Exp Brain Res 115:47–60.

Gray CM, McCormick DA (1996) Chattering cells: superficial pyramidal neurons contributing to the generation of synchronous oscillations in the visual cortex. Science 274:109–113.

Hattox AM, Nelson SB (2007) Layer V neurons in mouse cortex projecting to different targets have distinct physiological properties. J Neurophysiol 98:3330–3340.

Hefti BJ, Smith PH (2000) Anatomy, physiology, and synaptic responses of rat layer V auditory cortical cells and effects of intracellular $GABA_A$ blockade. J Neurophysiol 83:2626–2638.

Kampa BM, Letzkus JJ, Stuart GJ (2006) Cortical feed-forward networks for binding different streams of sensory information. Nat Neurosci 9:1472–1473.

Kawaguchi Y, Kubota Y (1997) GABAergic cell subtypes and their synaptic connections in rat frontal cortex. Cereb Cortex 7:476–486.

Killackey HP, Koralek KA, Chiaia NL, Rhodes RW (1989) Laminar and areal differences in the origin of the subcortical projection neurons of the rat somatosensory cortex. J Comp Neurol 282:428–445.

Kim J, Alger BE (2001) Random response fluctuations lead to spurious paired-pulse facilitation. J Neurosci 21:9608–9618.

Koester HJ, Johnston D (2005) Target cell-dependent normalization of transmitter release at neocortical synapses. Science 308:863–866.

Letzkus JJ, Kampa BM, Stuart GJ (2006) Learning rules for spike timing-dependent plasticity depend on dendritic synapse location. J Neurosci 26:10420–10429.

Lévesque M, Charara A, Gagnon S, Parent A, Deschênes M (1996) Corticostriatal projections from layer V cells in rat are collaterals of long-range corticofugal axons. Brain Res 709:311–315.

Lübke J, Feldmeyer D (2007) Excitatory signal flow and connectivity in a cortical column: focus on barrel cortex. Brain Struct Funct 212:3–17.

Markram H, Toledo-Rodriguez M, Wang Y, Gupta A, Silberberg G, Wu C (2004) Interneurons of the neocortical inhibitory system. Nat Rev Neurosci 5:793–807.

Mason A, Larkman A (1990) Correlations between morphology and electrophysiology of pyramidal neurons in slices of rat visual cortex. II. Electrophysiology. J Neurosci 10:1415–1428.

McCormick DA, Pape HC (1990) Properties of a hyperpolarization-activated cation current and its role in rhythmic oscillation in thalamic relay neurones. J Physiol 431:291–318.

McCormick DA, Connors BW, Lighthall JW, Prince DA (1985) Comparative electrophysiology of pyramidal and sparsely spiny stellate neurons of the neocortex. J Neurophysiol 54:782–806.

Morishima M, Kawaguchi Y (2006) Recurrent connection patterns of corticostriatal pyramidal cells in frontal cortex. J Neurosci 26:4394–4405.

Mountcastle VB (1997) The columnar organization of the neocortex. Brain 120:701–722.

Nuñez A, Amzica F, Steriade M (1993) Electrophysiology of cat association cortical cells in vivo: intrinsic properties and synaptic responses. J Neurophysiol 70:418–430.

Reiner A, Jiao Y, Del Mar N, Laverghetta AV, Lei WL (2003) Differential morphology of pyramidal tract-type and intratelencephalically projecting-type corticostriatal neurons and their intrastriatal terminals in rats. J Comp Neurol 457:420–440.

Schubert D, Staiger JF, Cho N, Kötter R, Zilles K, Luhmann HJ (2001) Layer-specific intracolumnar and transcolumnar functional connectivity of layer V pyramidal cells in rat barrel cortex. J Neurosci 21:3580–3592.

Schubert D, Kötter R, Zilles K, Luhmann HJ, Staiger JF (2003) Cell type-specific circuits of cortical layer IV spiny neurons. J Neurosci 23:2961–2970.

Schubert D, Kötter R, Luhmann HJ, Staiger JF (2006) Morphology, electrophysiology and functional input connectivity of pyramidal neurons characterizes a genuine layer Va in the primary somatosensory cortex. Cereb Cortex 16:223–236.

Schwindt P, O'Brien JA, Crill W (1997) Quantitative analysis of firing properties of pyramidal neurons from layer 5 of rat sensorimotor cortex. J Neurophysiol 77:2484–2498.

Shepherd GM, Svoboda K (2005) Laminar and columnar organization of ascending excitatory projections to layer 2/3 pyramidal neurons in rat barrel cortex. J Neurosci 25:5670–5679.

Shepherd GM, Stepanyants A, Bureau I, Chklovskii D, Svoboda K (2005) Geometric and functional organization of cortical circuits. Nat Neurosci 8:782–790.

Sjöström PJ, Häusser M (2006) A cooperative switch determines the sign of synaptic plasticity in distal dendrites of neocortical pyramidal neurons. Neuron 51:227–238.

Song S, Sjöström PJ, Reigl M, Nelson S, Chklovskii DB (2005) Highly nonrandom features of synaptic connectivity in local cortical circuits. PLoS Biol 3:e68.

Su H, Alroy G, Kirson ED, Yaari Y (2001) Extracellular calcium modulates persistent sodium current-dependent burst-firing in hippocampal pyramidal neurons. J Neurosci 21:4173–4182.

Thomson AM, Bannister AP (1998) Postsynaptic pyramidal target selection by descending layer III pyramidal axons: dual intracellular recordings and biocytin filling in slices of rat neocortex. Neuroscience 84:669–683.

Tsiola A, Hamzei-Sichani F, Peterlin Z, Yuste R (2003) Quantitative morphologic classification of layer 5 neurons from mouse primary visual cortex. J Comp Neurol 461:415–428.

Wilson CJ (1987) Morphology and synaptic connections of crossed corticostriatal neurons in the rat. J Comp Neurol 263:567–580.

Wise SP, Jones EG (1977) Cells of origin and terminal distribution of descending projections of the rat somatic sensory cortex. J Comp Neurol 175:129–157.

Yoshimura Y, Callaway EM (2005) Fine-scale specificity of cortical networks depends on inhibitory cell type and connectivity. Nat Neurosci 8:1552–1559.

Yoshimura Y, Dantzker JL, Callaway EM (2005) Excitatory cortical neurons form fine-scale functional networks. Nature 433:868–873.